J. Cell. Mol. Med. Vol 15, No 5, 2011 pp. 1210-1224

The RNA binding protein Musashi1 regulates apoptosis, gene expression and stress granule formation in urothelial carcinoma cells

Parvaneh Nikpour [a, b], Modjtaba Emadi Baygi [c], Christine Steinhoff [d], Christiane Hader [e], Anna C. Luca [f], Seyed J. Mowla [a], Wolfgang A. Schulz [e, *]

[a] *Department of Genetics, Faculty of Biological Sciences, Tarbiat Modares University, Tehran, Iran*
[b] *Department of Genetics and Molecular Biology, Faculty of Medicine, Isfahan University of Medical Sciences, Isfahan, Iran*
[c] *Department of Genetics, Faculty of Basic Sciences, Shahrekord University, Shahrekord, Iran*
[d] *Max Planck Institute for Molecular Genetics, Department of Computational Molecular Biology, Berlin, Germany*
[e] *Department of Urology, Heinrich Heine University, Düsseldorf, Germany*
[f] *Department of Surgery, Heinrich Heine University, Düsseldorf, Germany*

Received: January 14, 2010; Accepted: April 17, 2010

Abstract

The RNA-binding protein Musashi1 (MSI1) is a marker of progenitor cells in the nervous system functioning as a translational repressor. We detected *MSI1* mRNA in several bladder carcinoma cell lines, but not in cultured normal uroepithelial cells, whereas the paralogous *MSI2* gene was broadly expressed. Knockdown of *MSI1* expression by siRNA induced apoptosis and a severe decline in cell numbers in 5637 bladder carcinoma cells. Microarray analysis of gene expression changes after *MSI1* knockdown significantly up-regulated 735 genes, but down-regulated only 31. Up-regulated mRNAs contained a highly significantly greater number and density of Musashi binding sites. Therefore, a much larger set of mRNAs may be regulated by Musashi1, which may affect not only their translation, but also their turnover. The study confirmed $p21^{CIP1}$ and Numb proteins as targets of Musashi1, suggesting additionally $p27^{KIP1}$ in cell-cycle regulation and Jagged-1 in Notch signalling. A significant number of up-regulated genes encoded components of stress granules (SGs), an organelle involved in translational regulation and mRNA turnover, and impacting on apoptosis. Accordingly, heat shock induced SG formation was augmented by Musashi1 down-regulation. Our data show that ectopic *MSI1* expression may contribute to tumorigenesis in selected bladder cancers through multiple mechanisms and reveal a previously unrecognized function of Musashi1 in the regulation of SG formation.

Keywords: Musashi gene family • bladder cancer • apoptosis • stress granules • translational regulation • gene expression microarray

Introduction

The Musashi family is an evolutionarily conserved group of RNA-binding proteins [1, 2] which in mammals comprises the Musashi1 and Musashi2 proteins, encoded by the *MSI1* and *MSI2* genes, [3, 4], resembling each other in their RNA-binding domains [4]. Musashi1 is mainly expressed in central nervous system (CNS) stem cells and neural progenitor cells [2], but also in stem cell-enriched regions of murine and human intestinal crypts and stomach pits [5–7] and in epithelial progenitors in gastric mucosa, gut, mammary glands, epidermis and hair follicles [2, 6, 8, 9]. In contrast, Musashi2 is expressed in a wide variety of tissues, although its expression in the CNS is cell type specific and developmentally regulated [4].

Musashi1 functions as a translational repressor through sequence-specific interaction with the 3′-untranslated region (UTR) of various target mRNAs [10]. The best-established targets of Musashi1 are regulators of Notch signalling and the cell cycle such as Numb [10], an evolutionary conserved antagonist of the Notch pathway. Therefore, Musashi1 is thought to activate Notch signalling required for the self-renewal of mammalian neural stem

*Correspondence to: Wolfgang A. SCHULZ,
Department of Urology, Heinrich Heine University,
Moorenstr. 5, 40225, Düsseldorf, Germany.
Tel.: (49) 211-81-18966
Fax: (49) 211-81-15846
E-mail: wolfgang.schulz@uni-duesseldorf.de

doi:10.1111/j.1582-4934.2010.01090.x

cells. Accordingly, in NIH-3T3 cells, Musashi1 induces transactivation of the Notch target gene, *Hes1* [2, 10]. Moreover, Musashi1 has been reported to repress translation of the cyclin-dependent kinase inhibitor $p21^{CIP1}$ [11], which is necessary for commitment of proliferating neural progenitor cells to cell-cycle exit and neuronal differentiation [12]. Musashi1 was shown to inhibit translation initiation of its target mRNAs by competing with eIF4G for PABP, thereby inhibiting the assembly of the 80S ribosome, and to move subsequently with the stalled translation pre-initiation complex to cytoplasmic microorganelles such as stress granules (SGs) [13].

Musashi1 expression has also been reported in a variety of tumour cells, including glioblastoma, retinoblastoma, endometrial carcinoma, colorectal carcinoma and hepatoma cell lines [14–20]. The function of Musashi in tumour cells, however, is not well understood. Presumably, it may contribute to the maintenance of the self-renewal capacity of tumour (stem) cells by enhancing Notch pathway activity and preventing $p21^{CIP1}$-induced cell-cycle arrest.

In this study, we detected expression of *MSI1* genes in several bladder carcinoma cell lines, but not proliferating normal uroepithelial cells. Using an RNAi strategy, we observed that Musashi1 down-regulation decreased tumour cell proliferation by promoting cell death. A microarray analysis revealed expected and potential novel Musashis1 targets in Notch signalling and cell-cycle regulation and an unexpected effect on formation of SGs after heat-shock treatment. Our study suggests that ectopic expression of Musashi1 contributes to carcinogenesis in some urothelial cancers through several mechanisms.

Methods and materials

Cell lines, cell culture, siRNA transfection and heat-shock treatment

Bladder carcinoma cell lines and normal uroepithelial cells were cultured as described [21]. For heat-shock treatment, cells on cover slips were floated in the culture dish in a pan of water at 44°C for 20 min. and immediately thereafter fixed with paraformaldehyde/methanol.

Double-stranded, short (21-mer) interfering RNA (siRNA) corresponding to *MSI1* mRNA and a control non-targeting siRNA (IR-siRNA) with the following sense and antisense sequences were purchased from MWG (Ebersberg, Germany):

MSI1 sense/antisense

GGAGAAAGUGUGUGAAAUUdTdT/ AAUUUCACACAUUUCUCCdTdT

Irrelevant: sense/antisense

CUGAUGCAGGUAAUCGCGUdTdT/ ACGCGAUUACCUGCAUCAGdTdT

Cells were transfected with 25 μM siRNA at 30–50% confluency using Lipofectamine™ RNAiMAX following the recommendations of the manufacturer (Invitrogen, Karlsruhe, Germany). For replication experiments, MSI1 siRNA #L-011338–00 and non-targeting control #D-001810–10-OS (Dharmacon, Schwerte, Germany) were used at 10 μM with the same transfection reagent. Unless otherwise indicated, all assays were performed 3 days later.

RNA extraction

Total RNA was isolated from sub-confluent cell cultures and cell lines using Qiazol reagent (Qiagen, Hilden, Germany) and purified *via* RNeasy columns (Qiagen). cDNA synthesis was performed with SuperScriptII reverse transcriptase (Promega, Mannheim, Germany) with oligo-dT primers as described [22].

DNA extraction

High molecular weight genomic DNA from cell lines was isolated using the blood and cell culture DNA kit (Qiagen) with additional proteinase K treatment.

Methylation analysis

Bisulphite treatment of 1 μg of DNA from each sample was performed with the EZ DNA Methylation-Gold Kit™ (Zymo Research Corp, USA, Freiburg, Germany) yielding 50 μl converted DNA from each sample. For bisulphite sequencing, PCR of the *MSI1* promoter was performed with specific primers (For: GTAGGGATTTGAGAGGGAAGA and Rev: AACAAACCATACTACCCCCTC), in a volume of 50 μl containing 150 μM deoxyribonucleotide triphosphates (dNTPs), 0.3 μM of each primer, 1× PCR buffer (Qiagen), 1.0 U Hot Star Taq polymerase (Qiagen) and 2 μl of converted DNA. The initial denaturing step at 94°C for 15 min. was followed by 37 cycles each consisting of a denaturing step at 95°C for 30 sec., primer annealing at 59°C for 30 sec. and a 45 sec. elongation step at 72°C. The final 72°C period was extended to 10 min. Subsequently, PCR products were verified by agarose gel electrophoresis and subcloned into the pCR4-TOPO vector (Invitrogen, Groningen, Netherlands). At least four clones for each sample were sequenced by standard methods, and the number of clones analysed was increased to eight, if heterogeneous methylation patterns were detected.

Cell proliferation assay

Viable cells were quantified using the Cell Titer-Glo Luminescent Cell Viability Assay (Promega) according to the manufacturer's instructions. Results were based on four different experiments.

Cell cycle analysis

For flow cytometry analysis, cells were harvested by trypsinization 72 hrs after transfection, washed with PBS, then stained with 50 μg/ml propidium iodide solution containing 0.1% triton X-100 and sodium citrate as described [23] and were analysed for cell-cycle distributions using a FACS Calibur instrument (Becton Dickinson, Heidelberg, Germany). Cell-cycle profiles were analysed using WinMDI version 2.8 software.

Caspase assays

Caspase-3 and -7 activities were measured in quadruplicate with the Caspase-Glo 3/7 reagents (Promega).

RT-PCR

Real-time RT-PCR assays were performed with the LightCycler II apparatus (Roche, Mannheim, Germany). Real-time RT-PCR for *ADAM19* [ADAM

metallopeptidase domain 19 (NCBI GeneID: 8728)], *APP1* [amyloid beta (A4) precursor protein (NCBI GeneID: 351)], *BNIP3* [BCL2/adenovirus E1B 19kDa interacting protein 3 (NCBI GeneID: 664)], *CCNL1* [cyclin L1 (NCBI GeneID: 57018)], *CDKN1B* [cyclin-dependent kinase inhibitor 1B (p27, Kip1) (NCBI GeneID: 1027)], *HEY1* [hairy/enhancer-of-split related with YRPW motif 1 (NCBI GeneID: 23462)], *HIP1* [huntingtin interacting protein 1 (NCBI GeneID: 3092)], *ITGB1* [integrin, beta 1 (NCBI GeneID: 3688)], *RRAS* [related RAS viral (r-ras) oncogene homolog (NCBI GeneID: 6237)], *TIA1* [TIA1 cytotoxic granule-associated RNA binding protein (NCBI GeneID: 7072)] and *TBP* [TATA box binding protein (NCBI GeneID: 6908)] mRNAs was performed with specific Quantitect primer assays (Qiagen) with the *QuantiTect SYBR Green PCR Kit* (Qiagen). Real-time RT-PCR for *JAG1* [jagged 1 (NCBI GeneID: 182)] was performed with TaqMan assays in the GeneAmp 5700 Sequence Detection System (Applied Biosystems, Darmstadt, Germany). Real-time RT-PCR for *MSI1* [musashi homolog 1 (NCBI GeneID: 4440)], *MSI2* [musashi homolog 2 (NCBI GeneID: 124540)], *CDKN1A* [cyclin-dependent kinase inhibitor 1A (p21, Cip1) (NCBI GeneID: 1026)], *NUMB* [numb homolog (Drosophila) (NCBI GeneID: 8650)], *HES1* [hairy and enhancer of split 1 (NCBI GeneID: 3280)], *SPRY2* [sprouty homolog 2 (NCBI GeneID: 10253)] and *GAPDH* [glyceraldehyde-3-phosphate dehydrogenase (NCBI GeneID: 2597)] mRNAs was done using specific primers (Table S1) with the LightCycler-FastStart DNA Master PLUS SYBR Green I kit (Roche) or the *QuantiTect SYBR Green PCR Kit* (Qiagen). Values are expressed as mean ± S.E.M.

Microarray analysis and evaluation

Linear T7 polymerase-based amplification of total RNA from the three independent irrelevant (IR)-treated and MSI1-treated 5637 cell cultures was performed essentially as previously described [24]. RNA samples were then hybridized in duplicate to HG-U133A GeneChips (Affymetrix, Berlin, Germany) according to the manufacturer's instructions. Images were processed with GeneChip® Operating Software (GCOS, Version 1.3, Affymetrix) and total intensity normalization was applied by normalizing all arrays to an average signal level of 500 counts. For further analysis we used R/Bioconductor [25–27]. Raw probe-set intensities were normalized transformed to log scale using robust multi-array average [28] available as a package in Bioconductor. For each experiment, it was assumed that the majority of gene expressions were not differential with regard to all other experiments on the same array type. For background subtraction the minimal signal intensity was subtracted, a probe-specific background correction was not applied. Probe-set intensities of each probe set were summarized by applying the Tukey's median polish method [29] after normalization. Normalized expression values were used for further analysis.

To determine differential expression, the multitest package was used [26]. Differential gene expression was determined by permutation test. All tests were adjusted for multiple testing applying Benjamini–Hochberg adjustments [30]. *P*-values of <0.05 were considered to indicate statistical significance. Original designations by the array supplier for significant genes were annotated using the ensembl (www.ensembl.org) and the information hyperlinked over proteins (iHOP) [31] databases. Gene ontology group and Kyoto Encyclopedia of Genes and Genomes (KEGG) pathway analyses were performed with the WebGestalt software [32].

Western blotting

Cells were lysed in RIPA buffer containing 1% triton X-100, 0.5% sodium deoxycholate, 0.1% sodium dodecyl sulphate and complete protease inhibitor cocktail. Lysates containing the equivalent of 30 μg protein per lane were electrophoresed using SDS-PAGE (12% polyacrylamide gel) and were blotted on Immobilon-P membranes (Millipore, Hamburg, Germany). Blots were blocked for 1 hr with 5% milk powder in phosphate-buffered saline tween (PBST) or 3% bovine serum albumin and 1% milk powder in tris-buffered saline (TBS). They were then probed with polyclonal antibodies against Musashi1 (1:500; Novus, Hiddenhausen, Germany), $p21^{CIP1}$ (1:500; BD Biosciences, Heidelberg, Germany), m-Numb (1:500, Santa Cruz, Heidelberg, Germany), Jagged-1 (1:1000; Santa Cruz), $p27^{KIP1}$ (1:1000, Santa Cruz) or α-Tubulin (1:10,000; Sigma-Aldrich, Munich, Germany) as a loading control and subsequently with the horseradish peroxidase conjugated appropriate secondary antibodies (1:5000 or 1:100,000 with the enhanced kit). Staining was visualized using an (advanced) ECL chemiluminescence kit (Amersham Biosciences, Freiburg, Germany) or Immun-Star WesternC Kit (Biorad, Munich, Germany).

Immunofluorescence detection of stress granules

Fixed cells were incubated for 1 hr in PBS containing 4% bovine serum albumin and 0.05% saponine and subsequently stained overnight with anti-TIA-1 (1:200, Santa Cruz) antibody. Thereafter, cells were washed 2× in PBS and labelled with secondary antibody (1:500, Alexa 488-coupled anti-goat IgG [Invitrogen]). DNA was detected using DAPI (4,6-diamidino-2-phenylindole, 1 mg/ml; Sigma-Aldrich). Stainings were evaluated with a Nikon Eclipse 200/400 microscope (Nikon, Düsseldorf, Germany) and NIS Elements D2–30 software. Percentages of cells harbouring $\geq$5 SGs were determined by analysis of $>$4 fields in two independent experiments for a minimum of each 500 cells counted.

Further statistical analyses

Unless indicated otherwise, Student's t-test was used for statistical analyses. All experiments were replicated three or four times.

Results

Expression and siRNA-mediated down-regulation of MSI1 in urothelial carcinoma cells

According to quantitative RT-PCR, 8 of 15 bladder carcinoma cell lines displayed *MSI1* expression, in particular 639v and 5637 (Fig. 1A). No expression of *MSI1* was observed in any of several examined primary cultures of normal uroepithelial cells. In contrast, expression of *MSI2* was observed in all examined cell lines as well as normal uroepithelial cells (Fig. 1B).

The mechanisms responsible for cell type specific expression of *MSI1* are unknown. Because developmental genes are often silenced by DNA methylation in non-expressing cells, we investigated a region in the proximal *MSI1* promoter by bisulphite sequencing. Four bladder carcinoma cell lines were compared to two independent primary cultures of normal uroepithelial cells. The 55 CpG sites located close to the transcriptional start site were

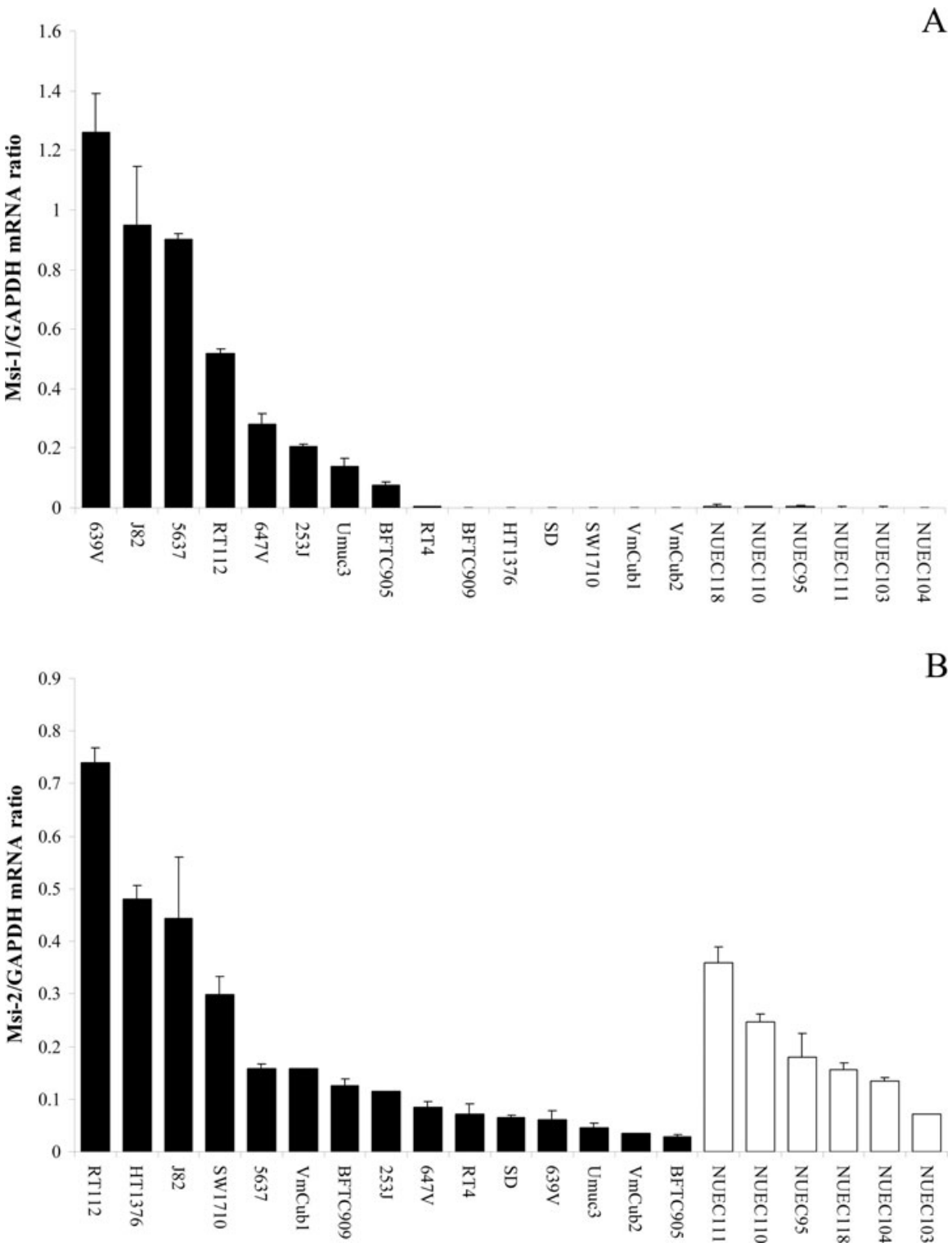

Fig. 1 Expression of *MSI1* and *MSI2* in bladder cancer cell lines and normal urothelial cells. Relative gene expression of *MSI1* to *GAPDH* (**A**) and *MSI2* to *GAPDH* (**B**) as determined by quantitative RT-PCR in bladder cancer cell lines (black columns) and several independent cultures of normal uroepithelial cells (NUECs, white columns). Values shown represent the mean ± S.E.M.

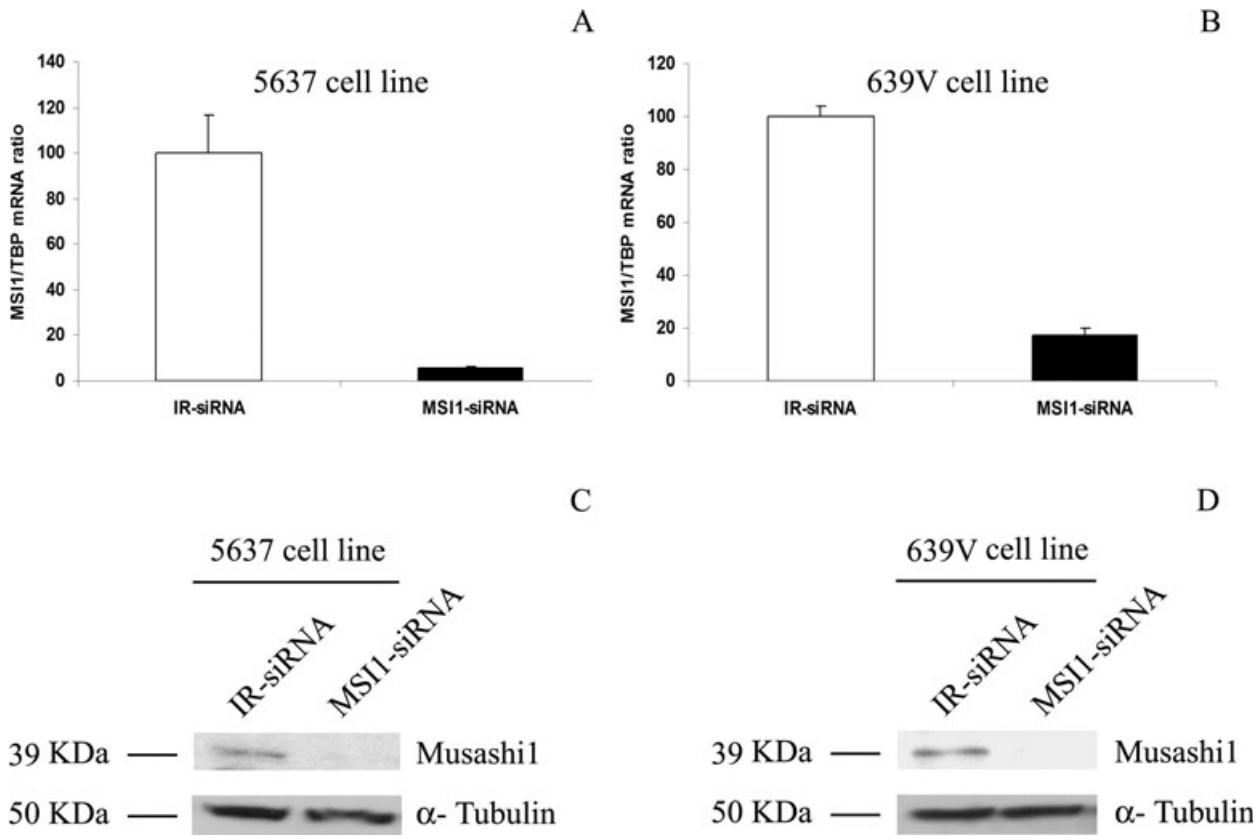

Fig. 2 Efficiency of down-regulation of *MSI1* expression by siRNA in bladder cancer cell lines. Expression of *MSI1* mRNA after 72 hrs of treatment with specific siRNA or control siRNA (IR) in 5637 (**A**) and 639v (**B**) cell lines as determined by quantitative RT-PCR. Relative expression in IR-siRNA treated cells was adjusted to 100. Effect on protein levels (**C** and **D**, respectively), as determined by Western blotting; α-tubulin was used as a loading control.

found completely unmethylated in normal uroepithelial cells, whereas SD and 5637 cells both exhibited partial methylation (Fig. S1), despite their very different expression levels of *MSI1* mRNA (Fig. 1A). These results suggest that DNA methylation is not a major factor in the silencing of *MSI1* in normal urothelial cells or cancer cell lines.

To investigate the function of Musashi1 by RNAi, we selected the 5637 and 639v cell lines, with high *MSI1* and low *MSI2* expression. Analysis by quantitative RT-PCR demonstrated that application of MSI1-siRNA for 3 days resulted in a dramatic reduction in *MSI1* mRNA expression by 94% and 83%, respectively, in 5637 and 639v cells compared to cells treated with an IR-siRNA (Fig. 2A and B). Strong down-regulation was already apparent after 24 hrs (data not shown). As shown by Western blotting, the reduction in *MSI1* mRNA was followed by a similar reduction at the protein level in MSI1-siRNA transfected 5637 and 639v cells (Fig. 2C and D). Down-regulation of MSI1 was accompanied by a moderate up-regulation of *MSI2* mRNA expression by 50% and 45%, respectively, in 5637 and 639v cells compared to cells treated with a control siRNA.

Effects of Musashi1 knockdown on cell proliferation and apoptosis

Three days after transfection, cell numbers, as measured by total ATP amounts, were diminished by 83% in MSI1-siRNA treated 5637 cells compared to cells treated with IR-siRNA ($3.3 \pm 0.5 \times 10^3$ *versus* $19.0 \pm 1.4 \times 10^3$, $P < 0.05$). After 1 and 2 days, ATP amounts were reduced by 30% and 40%, respectively. A weaker decrease, by 24%, was observed upon MSI1 down-regulation in 639v cells ($14.2 \pm 1.1 \times 10^4$ *versus* $18.7 \pm 1.2 \times 10^4$). No significant change was elicited by treating normal uroepithelial cells, which lack *MSI1* mRNA expression, with MSI1 siRNA ($33.4 \pm 0.7 \times 10^4$ *versus* $36.4 \pm 1.1 \times 10^4$).

In flow cytometry analysis in 5637 cells treated with MSI1- and IR-siRNAs, the fraction of cells appearing in 'sub-G1', indicative of apoptosis, increased significantly ($P < 0.05$) almost 2-fold from $4.6 \pm 0.1\%$ in MSI1-siRNA compared to IR-treated 5637 cells (Fig. 3A, upper panel). Treatment of 639v cells with MSI1-siRNA showed a much weaker and non-significant effect (Fig. 3B). Moreover, MSI1-siRNA treatment

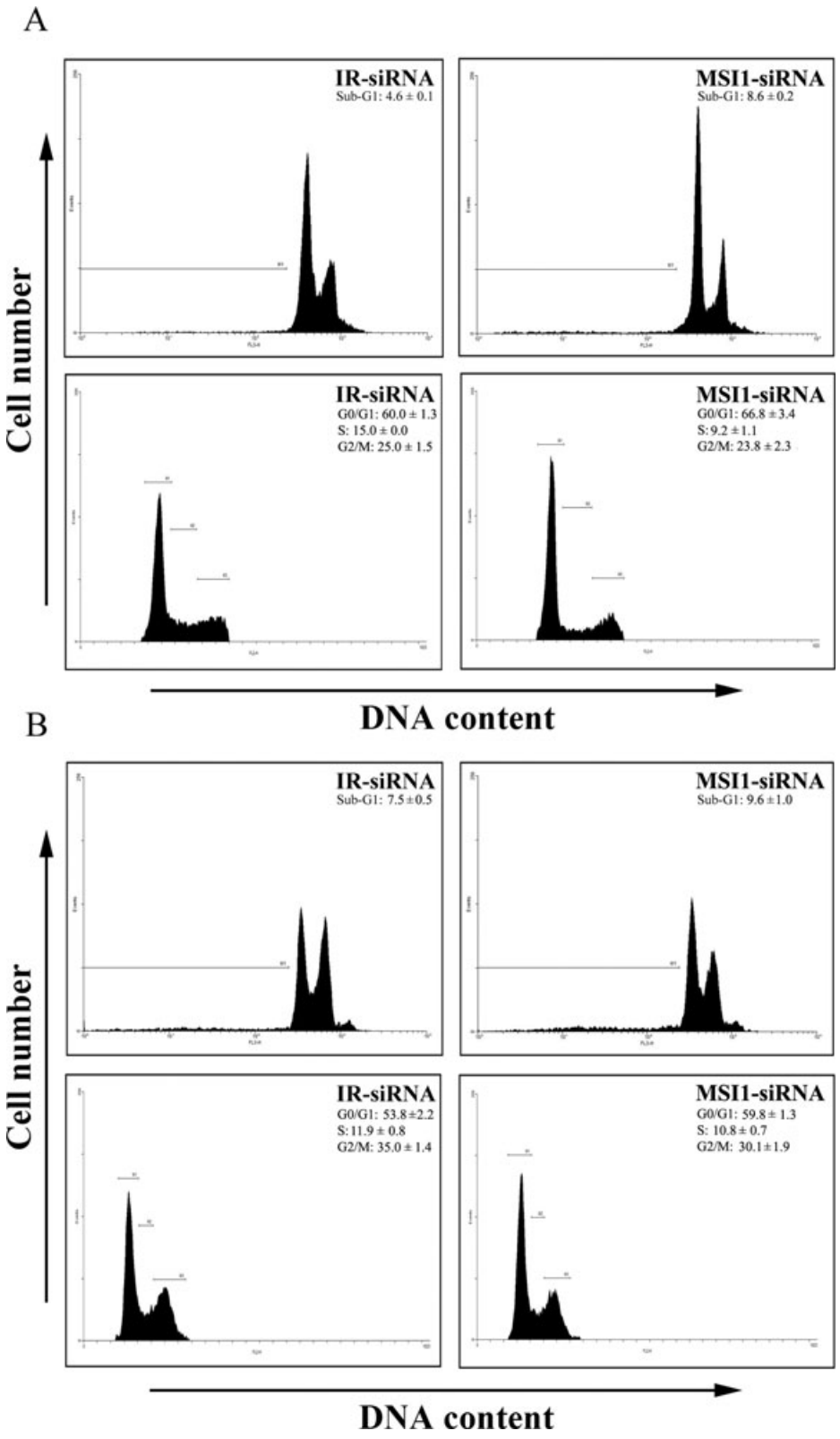

Fig. 3 Effect of MSI1 knockdown on cell-cycle distribution in bladder cancer cell lines. Cell-cycle distribution of 5637 (**A**) and 639v (**B**) cell lines after MSI1-siRNA treatment. The upper panels show the sub-G1 population of cells as depicted by the FL3 filter of the FACS instrument and the lower panels show the distribution and respective percentages of cells in the G0/G1, S and G2/M phases.

resulted in slightly, but not significantly increased G0/G1 fractions in both cell lines.

In accordance with the flow cytometry results, MSI1-siRNA treated 5637 cells showed a significant 4.8-fold elevation in the caspase-3 and caspase-7 activities compared to cells treated with IR-siRNA (0.45 ± 0.06 *versus* 0.09 ± 0.02, $P < 0.05$) after 3 days of treatment. Weaker increases were observed 1 and 2 days after MSI1-siRNA transfection (data not shown). In contrast, caspase-3 and caspase-7 activities in MSI1-siRNA *versus* IR-siRNA treated 639v cells were only slightly elevated (0.08 ± 0.01 *versus* 0.10 ± 0.001).

Effects of Musashi1 knockdown on gene expression

To examine how down-regulation of *MSI1* influenced gene expression, we performed a microarray experiment using HG-U133A oligonucleotide arrays. Of the approximately 13,000 genes represented on the array, 735 genes were significantly up-regulated at least 2-fold, but only 31 were down-regulated in a statistically significant manner after treatment of 5637 cells with MSI1-siRNA compared to IR-siRNA (Table S2).

Among the genes down-regulated by MSI1 siRNA treatment, several typically expressed in keratinocytes were conspicuous. Accordingly, the by far most significantly enriched gene ontology group among the 31 down-regulated genes was 'epidermis development' (Fisher's exact test: $P = 7 \times 10^{-6}$).

Among the much more numerous genes up-regulated after Musashi1 knockdown, a number of gene ontology (GO) groups were overrepresented (Table 1). According to this analysis, genes regulated by Musashi1 are involved in endoplasmic reticulum (ER) and Golgi function, protein secretion and protein ubiquitination, in signalling across the cell membrane through adhesion molecules and tyrosine kinase receptors, and in the regulation of cell proliferation. Notably, the GO groups 'positive regulation of cell proliferation', 'negative regulation of cell proliferation' as well as 'epithelial cell proliferation' were all significantly overrepresented. Unexpectedly in view of the overall effect of MSI1 knockdown on 5637 cells, a significant number of genes involved in 'negative regulation of apoptosis' were up-regulated. However, some pro-apoptotic genes also became strongly up-regulated, in particular *BNIP* and *BNIP3L* [33], by 3.2-fold and 4.7-fold, respectively.

Up-regulation of several cell cycle and cell death-related genes after *MSI1* depletion was confirmed by quantitative RT-PCR for *CDKN1A/p21*, *CDKN1B/p27*, *BNIP3*, *SPRY2* and *HPP1* transcripts (Fig. 4A). Likewise, according to Western blotting, $p21^{CIP1}$ and $p27^{KIP1}$ protein levels increased after *MSI1* down-regulation in 5637 cells, but notably not in 639v cells (Fig. 4B).

Although the KEGG pathway 'Notch signalling' comprising 46 genes was not overrepresented as a whole among the genes more than 2-fold up-regulated by *MSI1* knockdown, several genes were affected more than 1.5-fold, *i.e. CTBP2*, *PSEN1* and *ADAM17* and the well-characterized Musashi1 target *NUMB* [10], and *JAG1* and *ADAM19* were up-regulated 3.8- and 4.6-fold, respectively. Measurement of the mRNA levels of selected components of Notch pathway by RT-PCR confirmed these changes (Fig. 5A). The prototypical Notch pathway target gene *HEY1* was also induced, but not *HES1*. A separate time course experiment showed that the differences between cells transfected with MSI1-siRNA and IR-siRNA in the mRNA levels of *JAG1* and *ADAM19* increased over three consecutive days (data not shown). Moreover, we confirmed that Numb and Jagged-1 protein levels increased after *MSI1* down-regulation in 5637 cells, but not in 639v cells (Fig. 5B). Of note, the amounts of full-length Jagged-1 protein, appearing as a double band around 150 kD as well as of a smaller approximately 20 kD band, representing a C-terminal fragment of Jagged-1 resulting from proteolytic cleavage by ADAM17 [34], were augmented.

Several of the above experiments were independently repeated using MSI1 and control siRNAs from another commercial source. Key findings were replicated, including gradual induction of apoptosis and up-regulation of *ADAM19*, *CDKN1B*, *JAG1*, *NUMB*, *RRAS* and *SPRY2* mRNA after *MSI1* knockdown (data not shown).

Effects of Musashi1 knockdown on stress granules

Among the genes significantly up-regulated upon *MSI1* knockdown, we noted several reported to influence RNA stability and turnover, such as *CCNL1* [35], *RRAS* [36], *APP1* [37] and *TIA-1* [38], which increased 2.1-, 3.1-, 2.9- and 3.1-fold, respectively, and in particular, some associated with SGs. Of 35 proteins listed as SG components in a recent review [39] encoded by genes represented on the microarray, 9 were significantly up-regulated following Musashi1 knockdown (Table 2). In addition, for five others, closely related genes or genes encoding subunits were up-regulated. Only four such genes would have been expected by chance. Quantitative RT-PCR confirmed up-regulation of *RRAS* (*P*-value = 0.0065) and *APP1* (*P*-value = 0.039) after MSI1 siRNA treatment, whereas up-regulation of *TIA-1* and *CCNL1* was much weaker than expected from the microarray data (Fig. 6). We therefore evaluated the effect of MSI1 depletion on the formation of SGs, which were detected by a specific antibody against TIA-1. After *MSI1* depletion, the number of 5637 cells forming several SGs after heat shock increased strongly and highly significantly compared to cells treated with IR-siRNA (Fig. 7). Intriguingly, 639v cells did not form SGs under either condition.

Bioinformatic analysis of Musashi1 binding sites in regulated mRNAs

We finally compared several relevant mRNA structural parameters between the 31 down-regulated and the 31 most strongly up-regulated genes after *MSI1* knockdown, namely the transcript length, the length of the 3′-UTR, the relative length of the 3′-UTR in relation to the overall transcript length, the number of MSI1 consensus binding sites ($(G/A)U_nAGU$ [$n = 1$~3]) per 3′-UTR of each transcript and the number of Musashi1 binding sites per relative length of 3′-UTR. Interestingly, every parameter showed a highly significant difference between up-regulated and down-regulated genes (Table 3).

Table 1 Gene ontology (GO) groups most overrepresented after MSI1 knockdown in 5637 cells

GO group name	GO group level*	No. of genes observed	No. of genes expected	P-value**
Golgi vesicle transport	8	19	5.8	0.000027
Enzyme-linked receptor protein signalling pathway	6	26	10.9	0.000115
ER to Golgi vesicle-mediated transport	9	14	4.1	0.000209
Regulation of cell proliferation	5	35	17.6	0.000238
Vesicle-mediated transport	5	36	19.4	0.000619
Cell organization and biogenesis	4	107	77.9	0.000648
Secretory pathway	5	23	10.7	0.00102
Cell motility	4	27	13.5	0.00105
Cellular localization	5	49	30.4	0.00128
Cell migration	5	15	5.8	0.00162
Establishment of cellular localization	6	48	30.1	0.00170
Intracellular transport	7	47	29.7	0.00226
Small GTPase-mediated signal transduction	6	32	15.9	0.00336
Negative regulation of programmed cell death	7	18	8.4	0.00372
Epithelial cell proliferation	5	4	0.5	0.00380
Protein ubiquitination	9	9	2.9	0.00455
Negative regulation of cell proliferation	6	19	9.3	0.00460
Positive regulation of cell proliferation	6	17	8.0	0.00505
Negative regulation of cellular physiological process	5	55	38.1	0.00582
Transmembrane receptor protein serine/threonine kinase signalling pathway	7	8	2.5	0.00609
Protein modification by small protein conjugation	8	9	3.1	0.00671
Negative regulation of apoptosis	8	17	8.3	0.00679
Transforming growth factor β receptor signalling pathway	8	7	2.0	0.00692
Transmembrane receptor protein tyrosine kinase signalling pathway	7	16	7.7	0.00740
Positive regulation of epithelial cell proliferation	7	3	0.3	0.00750
Positive regulation of cellular process	4	48	32.9	0.00846
Cell proliferation	4	46	31.5	0.00954

*Only GO groups at level >3 were considered.
**Fisher's exact test.

Discussion

Musashi1 is considered to be a key molecule for stemness in various tissues and its expression has also been linked to increased cell proliferation in breast and intestinal cancers [40]. Musashi1 might exert an oncogenic function through its ability to repress translation of specifically bound mRNAs, including those for regulators of Notch signalling and the cell cycle like Numb and $p21^{CIP1}$ [10, 11]. However, the oncogenic functions of Musashi1 are poorly understood to date.

In the present study, we observed expression of *MSI1* in a subset of bladder cancer cell lines, but never in normal uroepithelial cells, even though these proliferate robustly in culture. Therefore, as observed in other cancer types, some urothelial cancers may ectopically express *MSI1*. The major effect of siRNA-mediated down-regulation in two bladder cancer cell lines was increased apoptosis, which was considerably more pronounced in the 5637 cell line, with only a slight increase in the G1/G0 fraction. The fact that no significant change in cell viability was observed in MSI1-siRNA treated normal uroepithelial cells excludes off-target effects of the treatment. An elevated apoptotic rate following *MSI1* suppression was also observed in some previous studies on other cell types [17, 41], but not generally [11, 42]. Moreover, overexpression of *Msi1* stimulated proliferation and increased S and G2/M

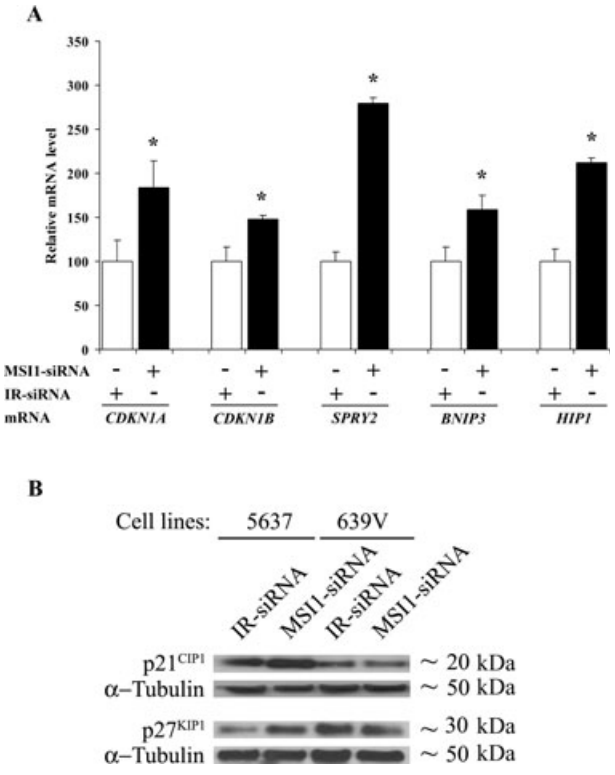

Fig. 4 Expression of selected growth regulatory genes in MSI1-siRNA treated cells. (**A**) Expression of *CDKN1A*, *CDKN1B*, *BNIP3*, *HIP* and *SPRY2* relative to *TBP* in the bladder cancer cell line 5637 after successful suppression of *MSI1* (see first bar on the left) as determined by quantitative RT-PCR. For each gene, relative expression in IR-siRNA treated controls was adjusted to 100. (**B**) Western blot analysis of $p21^{CIP1}$ and $p27^{KIP1}$ expression following MSI1 siRNA treatment in the bladder cancer cell lines 5637 and 639v; α-tubulin was employed as a loading control. Statistically significant differences ($P < 0.05$) are marked by asterisks.

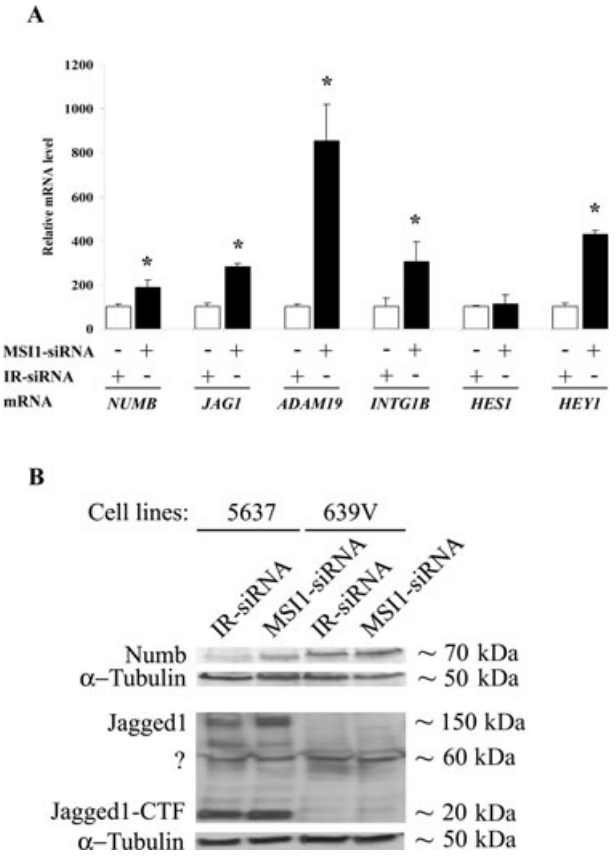

Fig. 5 Expression of selected Notch signalling related genes in MSI1-siRNA treated cells. (**A**) Expression of *NUMB*, *JAG1*, *ADAM19*, *INTG1B*, *HES1* and *HEY1* relative to *TBP* in the bladder cancer cell line 5637 after suppression of MSI1 as determined by quantitative RT-PCR. For each gene, the relative expression in IR-siRNA treated controls was adjusted to 100. Statistically significant differences ($P < 0.05$) are marked by asterisks. (**B**) Western blot analysis of Numb and Jagged-1 expression, with α-tubulin as a loading control. Note that the intensity of both the bands representing full-length Jagged-1 protein (around 150 kD) and the 20 kD C-terminal fragment were increased after MSI1 suppression in 5637 cells and the lack of Jagged-1 in 639v cells under either condition. The identity of the 60 kD band in the Jagged-1 blot is unknown.

fractions in a mouse mammary epithelial cell line [43] and human embryonic kidney cells [11]. In the human colon cancer cell line HCT116 too, knockdown of *MSI1* decreased the fraction of actively cycling cells [17]. Considering these results together, it seems that effects of *MSI1* on cell-cycle distribution occur in a cell-context dependent manner. An explanation for the various outcomes is suggested by the result of our microarray analysis that *MSI1* knockdown increased the expression of both proliferation inhibitory and stimulatory genes in 5637 (Table 1). The ultimate effect of *MSI1* may therefore depend on how the balance between these genes turns out in a particular cell type. In a similar fashion, both anti-apoptotic and pro-apoptotic genes turned out to be influenced by *MSI1* in our analysis. Although a significant number of genes involved in negative regulation of apoptosis were up-regulated after MSI1-siRNA treatment, two pro-apoptotic genes, *BNIP* and *BNIP3L*, encoding NIP3 and NIX (NIP-like protein X) [33] became induced too. They are possible candidates for mediating apoptosis in 5637 cells in response to *MSI1* knockdown. In addition, although $p21^{CIP1}$ and $p27^{KIP1}$, which were up-regulated under that condition are often anti-apoptotic, they can promote apoptosis under certain conditions [44, 45], presumably because apoptosis frequently occurs in cells in the G1 phase of the cell cycle [46, 47], and arrest in late G1 or S phase mediated by the cell-cycle inhibitors can then accelerate or potentiate apoptosis [48]. However, the mechanism of apoptosis in this case could be more complex, as suggested below.

In accordance with previous work [10, 11], we observed up-regulation of both Numb and $p21^{CIP1}$ proteins after *MSI1* down-regulation in 5637 cells. Our findings, however, may extend present knowledge in several respects (summarized in Fig. 8).

Table 2 SG-related proteins as cited in Ref. [39] and their expression changes after MSI1 knockdown

Protein	Gene symbol	Related gene(s)	Expression changes after MSI1 knockdown	Fold change	Adjusted *P*-value
Ago2	*EIF2C2*		No change		
APOBEC3G	*APOBEC3G*		Up-regulated	2.41	0.018
Ataxin-2	*ATXN2*		No change		
Caprin-1	*GPIAP1*		Not present		
CPEB	*CPEB1*		No change		
DISC1	*DISC1*		No change		
eIF3		*EIF3A*	Up-regulated	2.83	0.028
eIF4E	*eIF4E*		Up-regulated	2.45	0.028
eIF4G	*EIF4G1*		Up-regulated	1.63	0.035
FAST	*FASTK*	*FASTKD3*	Up-regulated	1.62	0.046
FMRP	*FMR1*		No change		
FXR1	*FXR1*		Up-regulated	2.60	0.018
FBP	*FUBP1*	*FUBP3*	Up-regulated	2.94	0.028
KSRP	*KHSRP*		No change		
G3BP	*G3BP*	*G3BP2*	Up-regulated	2.37	0.035
HuR	*ELAVL1*		No change		
IP5K	*IPPK*		No change		
Lin28	*LIN28*		No change		
LINE 1 ORF1p	*LRE1*		Not present		
MLN51	*CASC3*		No change		
PABP-1	*PABPC1*		No change		
RCK (p54)	*DDX6*		No change		
Plakophilin	*PKP1*		No change		
PMR1	*ATP2C1*		Up-regulated	1.87	0.035
Pumilio 2	*PUM2*		Up-regulated	1.66	0.018
Rap 55	*LSM14A*		Up-regulated	3.01	0.018
Rpb 4	*POLR2D*	*POLR2K*	Up-regulated	1.98	0.028
SRC3	*NCOA3*		No change		
Staufen	*STAU1*		No change		
SMN	*SMN1*		No change		
TIA-1	*TIA1*		Up-regulated	3.07	0.018
TIAR	*TIAL1*		No change		
TRAF2	*TRAF2*		No change		
TTP	*ZFP36*		No change		
BRF1	*ZFP36L1*		Up-regulated	1.87	0.028
YB-1	*YBX1*		No change		
ZBP-1	*ZBP1*		No change		

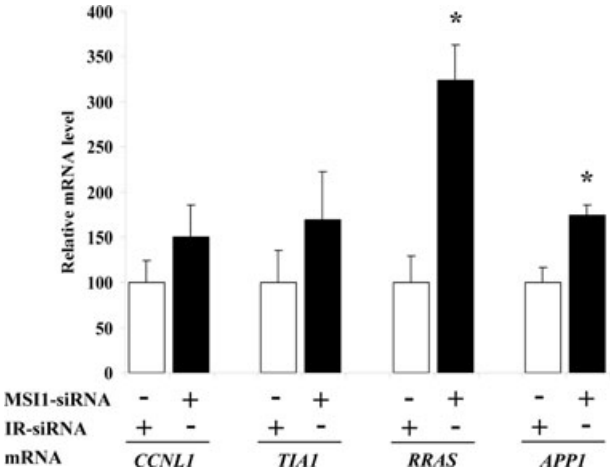

Fig. 6 Expression of genes related to RNA turnover in MSI1-siRNA treated 5637 cells. Expression of *CCNL1*, *TIA1*, *RRAS* and *APP1* relative to *TBP* in the bladder cancer cell line 5637 after suppression of *MSI1* as determined by quantitative RT-PCR. In all cases, the relative expression of each gene in IR-siRNA treated controls was adjusted to 100. Statistically significant differences ($P < 0.05$) are marked by asterisks.

First, we observed that not only the levels of Numb and p21^{CIP1} proteins, but also the levels of their corresponding mRNAs were elevated, suggesting that translational inhibition by Musashi1 also affects the turnover of the respective mRNAs. A plausible explanation for this effect is the recent finding that Musashi1 elicits the transport of its target mRNAs to particles in the cell that sort RNAs for reuse, storage or degradation [13]. Interestingly, TIA-1 has a similarly dual role as a suppressor of translation as well as a regulator of the decay of selected mRNAs [38].

Second, our siRNA study, in accordance with another investigation employing *MSI1* overexpression [43] suggests that the range of Musashi1 targets may be much wider than hitherto recognized. Although it is not trivial to distinguish between direct effects of Musashi1 on mRNAs and effects elicited by secondary changes in transcription, two arguments support the idea that a substantial fraction of the genes identified as up-regulated in the microarray study (Table S2) are direct Musashi1 targets. A comparison of the RNA structures of the most strongly up-regulated and down-regulated genes showed that the up-regulated mRNAs had significantly longer 3′-UTRs and significantly more predicted binding sites overall and per unit of length, for Musashi1 protein. Moreover, secondary transcriptional changes would be expected to result in a similar number of up-regulated and down-regulated genes, whereas we observed a huge excess of up-regulated mRNAs, as one might expect after removal of a protein promoting mRNA turnover.

Third, our study suggests that *MSI1* effects on cell-cycle regulation and Notch signalling may be mediated not only by p21^{CIP1} and Numb, respectively. Although we did not find a significant overall enrichment of cell cycle regulatory or Notch pathway

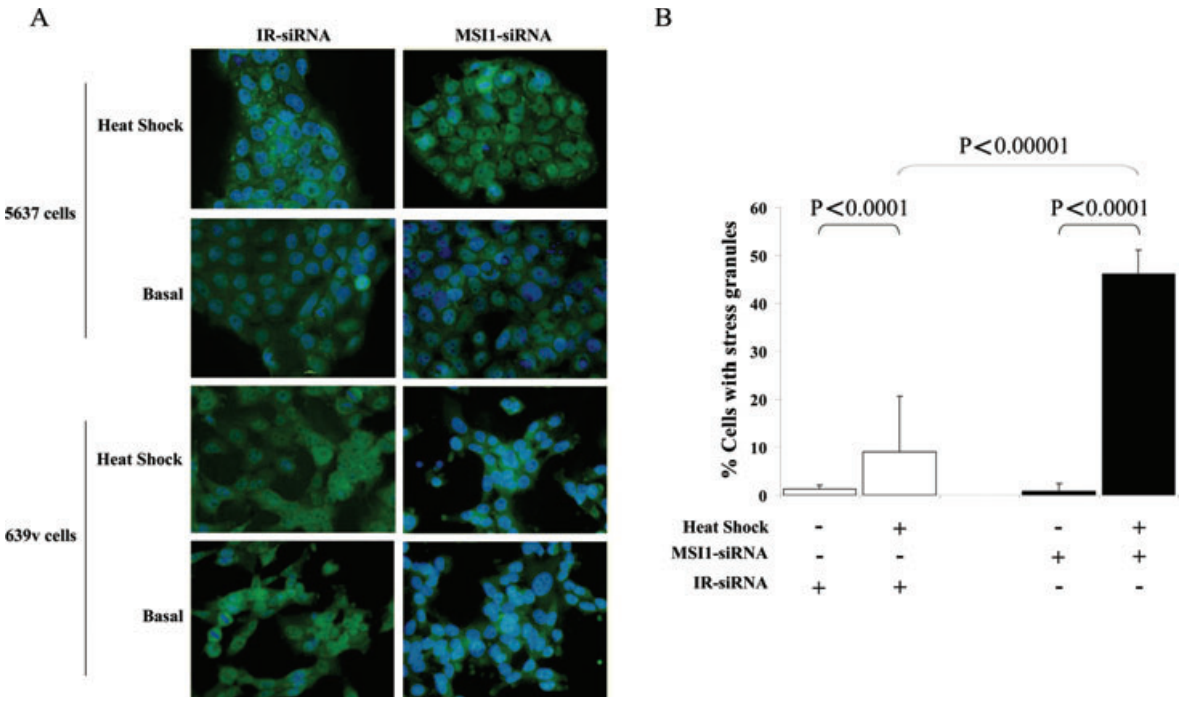

Fig. 7 Effect of MSI1 depletion on formation of SGs in bladder cancer cell lines 5637 and 639v. (**A**) SGs are visualized as distinctive irregularly shaped speckles after immunocytochemical staining for TIA-1. Note the absence of SGs under either condition in 639v cells. (**B**) Number of 5637 cells with >5 SGs under the indicated conditions. Statistically significant differences are indicated.

Table 3 Comparison of mRNA structural parameters between the 31 most down and up-regulated mRNAs after MSI1 knockdown

Genes status after MSI1 suppression	Mean transcript length (bps)	Mean 3′-UTR length (bps)	Mean relative length of 3′-UTR (in relation to total length)	Mean number of MSI1 binding sites per 3′-UTR	Mean number of MSI1 binding sites per relative length of 3′-UTR
Up-regulated	3714 ± 1774	1755 ± 1129	0.47 ± 0.21	4 ± 3.38	8.56 ± 7.38
Down-regulated	2043 ± 1522	646 ± 872	0.26 ± 0.16	0.71 ± 1.16	2.31 ± 3.61
P-value for difference (t-test)	2.22×10^{-4}	0.75×10^{-4}	0.55×10^{-4}	0.13×10^{-4}	2.20×10^{-4}

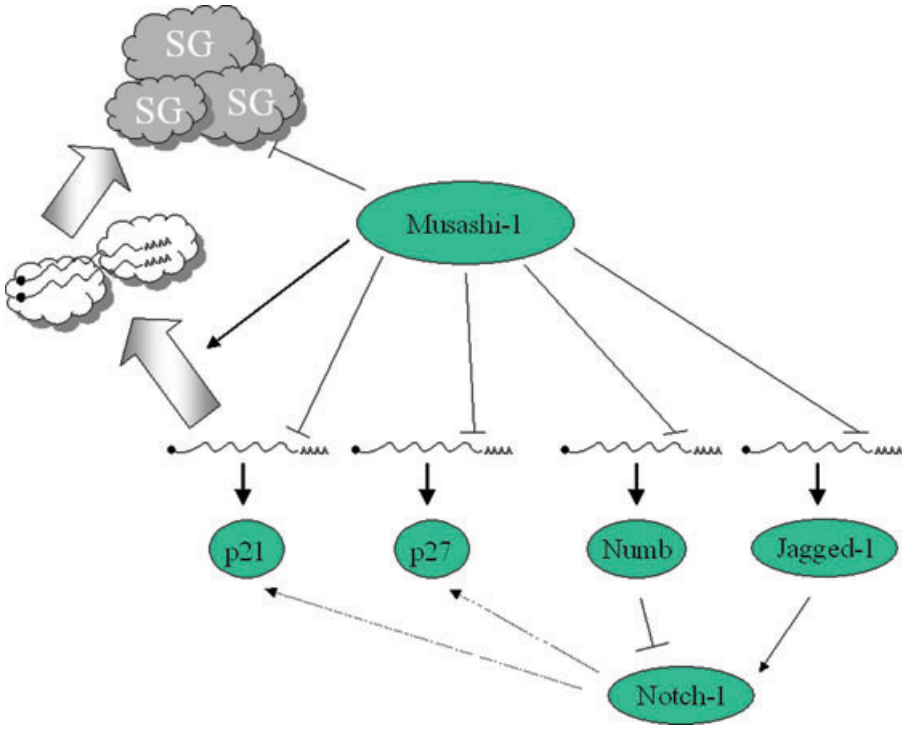

Fig. 8 Some aspects of Musashi1 function in urothelial carcinoma cells. Musashi1 is suggested to block translation of proteins involved in cell cycle and Notch signalling regulation and facilitate sequestration of the corresponding mRNAs to particles storing or degrading RNA. However, formation of SGs, which derive partly from such particles [39], under conditions of cellular stress is prohibited by Musashi1.

genes in the bioinformatic analysis of the microarray results, several additional genes in these regulatory systems were clearly influenced by *MSI1* knockdown. In cell-cycle regulation, at least $p27^{KIP1}$ was up-regulated in addition to $p21^{CIP1}$ at both mRNA and protein levels. We also confirmed up-regulation of the Notch ligand Jagged-1 mRNA and protein in 5637 following Musashi1 depletion. The finding that several proteins involved in Notch signalling are affected by Musashi1 may provide one explanation why we did not observe a full-scale effect of MSI1 knockdown on Notch signalling, *e.g.* induction of only *HEY1*, but not *HES1*, among the prototypic Notch target genes. There are moreover indications that Notch signalling in urothelial carcinomas may be generally defective, as Notch proteins may be down-regulated in this cancer type [49]. In accordance, in our study, we observed that 639v lacks Jagged-1 expression. Nevertheless, the effects on Numb, Jagged-1, *HEY1* and ADAM proteases observed in the present study underline the role of Musashi1 as a regulator of Notch signalling and indicate that further studies examining the interaction of MSI1 with other Notch pathway components are warranted.

Finally, unexpectedly, a significant number of genes encoding SG components were observed to become up-regulated after *MSI1* knockdown in our microarray study. We found that the formation of SGs after heat-shock treatment in 5637 cells was significantly facilitated by MSI1 depletion indicating that the high expression level of *MSI1* in 5637 cells impaired the formation of SGs. In this respect, our data show striking parallels to a recent report clarifying the role of mammalian Staufen 1, a double-stranded RNA-binding protein, in the formation of SGs [50]. Like Musashi1, Staufen 1 is also recruited into SGs [13] but its high expression impaired the assembly of SGs. Moreover, depletion of Staufen 1 also led to pronounced cell death [50]. These

findings fit with earlier indications that SGs can influence apoptosis in several situations [51]. Thus, like Staufen 1, Musashi1 may not only interact with RNA processing bodies like SGs in the course of its regulating translation of specific mRNAs, but also may regulate the very formation of these bodies. Such a function could account for the broad range of mRNAs affected by MSI1 knockdown and for its overall function on cell fate, proliferation and survival.

Throughout our study, we observed remarkable differences in the response to Musashi1 knockdown between the two bladder cancer cell lines 5637 and 639v (*e.g.* Figs 4, 5 and 7), despite their very similar initial levels of *MSI1* and efficiencies of Musashi1 knockdown (*cf.* Figs 1A and 2). It is unlikely that the differences are caused by Musashi2 compensating, as *MSI2* expression is lower in 639v than in 5637 (Fig. 1B) and the percentage increase after MSI1-siRNA treatment was similar. This increase in *MSI2* and other changes, including a pronounced increase in *HEY1* expression, illustrate that Musashi1 knockdown did elicit certain effects in 639v, although these did not result in major changes of apoptosis or cell-cycle distribution. A known difference between the cell lines that may influence their propensity towards apoptosis is the overexpression of E2F3 in 5637, due to a gene amplification [52], in comparison to 639v. In any case, the difference between the cell lines highlights again the cell-context specific action of Musashi1. Obviously, the ultimate effect of a translational regulator depends strongly on whether its mRNA targets are transcribed at all. The example of Jagged-1 (Fig. 5B) which is not expressed in 639v illustrates this argument. More generally, it is tempting to speculate that the weaker effects of Musashi1 in 639v cells may be related to the inability of these cells to form SGs. Conceivably, one or more essential factors required for their assembly may differ between 5637 and 639v. The cell pair, which otherwise shares many typical genetic defects of invasive bladder cancers, may therefore provide a good experimental system to identify factors cooperating with and regulating Musashi function and SG formation.

An important open question emerging from our study is to which extent Musashi1 expression may contribute to bladder cancer development. The bladder cancer cell lines used contain typical genetic and epigenetic aberrations of invasive urothelial cancers. A subset of them expressed, whereas others lacked *MSI* mRNA. We have accordingly observed a wide variation of *MSI1* mRNA expression in bladder cancer tissue samples (Nikpour *et al.*, unpublished data). This suggests that Musashi1 may also be relevant for survival and growth of selected urothelial cancers in the patients. Given the potential link of Musashi1 to stem cell function, a future assessment of the importance of Musashi1 *in vivo* will most of all require the identification of the cell types within the urothelial tumours that express the protein.

In summary, our results support the idea that *MSI1* functions as a regulator of cell proliferation and apoptosis in certain cancer cells. Our data confirm that regulators of the cell cycle and of Notch signalling are regulated by Musashi1. Furthermore, our data suggest that a much larger set of mRNAs are Musashi1 targets, and that the protein may regulate not only their translation, but also their turnover. In these functions, mutual interactions with RNA processing microorganelles, such as SGs, appear to be highly relevant.

Acknowledgements

We thank Dr. Nicolas Stoecklein for kindly providing the Numb antibody and primers. P.N. was supported partially by the Christiane and Claudia Hempel-Stiftung. C.S. is supported by FastTrack (Robert Bosch Foundation) and EuTRACC (Integrated Project, grant no. LSHG-CT-2007-037445).

Conflict of interest

The authors confirm that there are no conflicts of interest.

Supporting Information

Additional Supporting Information may be found in the online version of this article:

Fig. S1 Analysis of *MSI1* methylation. Bisulphite sequencing of the *MSI1* promoter region in selected cell lines and two independent urothelial cell cultures (NUECs). The localization of the 55 investigated CpG sites relative to the transcriptional start site is indicated on top; the black arrows represent location and direction of the bisulphite sequencing primers. Black and white cycles denote methylated and unmethylated CpG sites, respectively. The signs in parentheses indicate corresponding relative mRNA expression levels: [−] no or low expression and [+++] high expression.

Table S1 Sequences of primers for real-time RT-PCR

Table S2 Genes up-regulated or down-regulated after MSI1 knockdown according to microarray analysis

Please note: Wiley-Blackwell are not responsible for the content or functionality of any supporting materials supplied by the authors. Any queries (other than missing material) should be directed to the corresponding author for the article.

References

1. **Okano H, Imai T, Okabe M.** Musashi: a translational regulator of cell fate. *J Cell Sci*. 2002; 115: 1355–9.
2. **Okano H, Kawahara H, Toriya M, *et al*.** Function of RNA-binding protein Musashi-1 in stem cells. *Exp Cell Res*. 2005; 306: 349–56.
3. **Good P, Yoda A, Sakakibara S, *et al*.** The human Musashi homolog 1 (MSI1) gene encoding the homologue of Musashi/Nrp-1, a neural RNA-binding protein putatively expressed in CNS stem cells and neural progenitor cells. *Genomics*. 1998; 52: 382–4.
4. **Sakakibara S, Nakamura Y, Satoh H, *et al*.** Rna-binding protein Musashi2: developmentally regulated expression in neural precursor cells and subpopulations of neurons in mammalian CNS. *J Neurosci*. 2001; 21: 8091–107.
5. **Kayahara T, Sawada M, Takaishi S, *et al*.** Candidate markers for stem and early progenitor cells, Musashi-1 and Hes1, are expressed in crypt base columnar cells of mouse small intestine. *FEBS Lett*. 2003; 535: 131–5.
6. **Potten CS, Booth C, Tudor GL, *et al*.** Identification of a putative intestinal stem cell and early lineage marker; musashi-1. *Differentiation*. 2003; 71: 28–41.
7. **Akasaka Y, Saikawa Y, Fujita K, *et al*.** Expression of a candidate marker for progenitor cells, Musashi-1, in the proliferative regions of human antrum and its decreased expression in intestinal metaplasia. *Histopathology*. 2005; 47: 348–56.
8. **Clarke RB, Spence K, Anderson E, *et al*.** A putative human breast stem cell population is enriched for steroid receptor-positive cells. *Dev Biol*. 2005; 277: 443–56.
9. **Sugiyama-Nakagiri Y, Akiyama M, Shibata S, *et al*.** Expression of RNA-binding protein Musashi in hair follicle development and hair cycle progression. *Am J Pathol*. 2006; 168: 80–92.
10. **Imai T, Tokunaga A, Yoshida T, *et al*.** The neural RNA-binding protein Musashi1 translationally regulates mammalian numb gene expression by interacting with its mRNA. *Mol Cell Biol*. 2001; 21: 3888–900.
11. **Battelli C, Nikopoulos GN, Mitchell JG, *et al*.** The RNA-binding protein Musashi-1 regulates neural development through the translational repression of p21WAF-1. *Mol Cell Neurosci*. 2006; 31: 85–96.
12. **Erhardt JA, Pittman RN.** Ectopic p21(WAF1) expression induces differentiation-specific cell cycle changes in PC12 cells characteristic of nerve growth factor treatment. *J Biol Chem*. 1998; 273: 23517–23.
13. **Kawahara H, Imai T, Imataka H, *et al*.** Neural RNA-binding protein Musashi1 inhibits translation initiation by competing with eIF4G for PABP. *J Cell Biol*. 2008; 181: 639–53.
14. **Hemmati HD, Nakano I, Lazareff JA, *et al*.** Cancerous stem cells can arise from pediatric brain tumors. *Proc Nat Acad Sci USA*. 2003; 100: 15178–83.
15. **Seigel GM, Hackam AS, Ganguly A, *et al*.** Human embryonic and neuronal stem cell markers in retinoblastoma. *Mol Vis*. 2007; 13: 823–32.
16. **Gotte M, Wolf M, Staebler A, *et al*.** Increased expression of the adult stem cell marker Musashi-1 in endometriosis and endometrial carcinoma. *J Pathol*. 2008; 215: 317–29.
17. **Sureban SM, May R, George RJ, *et al*.** Knockdown of RNA binding protein musashi-1 leads to tumor regression *in vivo*. *Gastroenterology*. 2008; 134: 1448–58.
18. **Nakano A, Kanemura Y, Mori K, *et al*.** Expression of the Neural RNA-binding protein Musashi1 in pediatric brain tumors. *Pediatr Neurosurg*. 2007; 43: 279–84.
19. **Toda M, Iizuka Y, Yu W, *et al*.** Expression of the neural RNA-binding protein Musashi1 in human gliomas. *Glia*. 2001; 34: 1–7.
20. **Shu HJ, Saito T, Watanabe H, *et al*.** Expression of the Musashi1 gene encoding the RNA-binding protein in human hepatoma cell lines. *Biochem Biophys Res Commun*. 2002; 293: 150–4.
21. **Swiatkowski S, Seifert HH, Steinhoff C, *et al*.** Activities of MAP-kinase pathways in normal uroepithelial cells and urothelial carcinoma cell lines. *Exp Cell Res*. 2003; 282: 48–57.
22. **Hoffmann MJ, Muller M, Engers R, *et al*.** Epigenetic control of CTCFL/BORIS and OCT4 expression in urogenital malignancies. *Biochem Pharmacol*. 2006; 72: 1577–88.
23. **Janssen K, Pohlmann S, Janicke RU, *et al*.** Apaf-1 and caspase-9 deficiency prevents apoptosis in a Bax-controlled pathway and promotes clonogenic survival during paclitaxel treatment. *Blood*. 2007; 110: 3662–72.
24. **Kenzelmann M, Klaren R, Hergenhahn M, *et al*.** High-accuracy amplification of nanogram total RNA amounts for gene profiling. *Genomics*. 2004; 83: 550–8.
25. **Ihaka R, Gentleman R.** R: a language for data analysis and graphics. *J Comput Graph Stat*. 1996; 5: 299–314.
26. **Gentleman R, Carey V, Bates D, *et al*.** Bioconductor: Open software development for computational biology and bioinformatics. *Genome Biol*. 2004; 5: R80.
27. **Rainer J, Sanchez-Cabo F, Stocker G, *et al*.** CARMAweb: comprehensive R- and bioconductor-based web service for microarray data analysis. *Nucl Acids Res*. 2006; 34: W498–503.
28. **Bolstad B, Irizarry R, Astrand M, *et al*.** A comparison of normalization methods for high density oligonucleotide array data based on variance and bias. *Bioinformatics*. 2003; 19: 185–93.
29. **Tukey JW.** Exploratory data analysis. Reading, MA: Addison-Wesley; 1977.
30. **Benjamini Y, Hochberg Y.** Controlling the false discovery rate: a practical and powerful approach to multiple testing. *J Royal Stat Soc B*. 1995; 57: 289–300.
31. **Hoffmann R, Valencia A.** Implementing the iHOP concept for navigation of biomedical literature. *Bioinformatics*. 2005; 21: ii252–8.
32. **Zhang B, Kirov S, Snoddy J.** WebGestalt: an integrated system for exploring gene sets in various biological contexts. *Nucl Acids Res*. 2005; 33: W741–8.
33. **Chen G, Cizeau J, Vande Velde C, *et al*.** Nix and Nip3 form a subfamily of pro-apoptotic mitochondrial proteins. *J Biol Chem*. 1999; 274: 7–10.
34. **LaVoie MJ, Selkoe DJ.** The Notch ligands, Jagged and Delta, are sequentially processed by alpha-secretase and presenilin/gamma-secretase and release signaling fragments. *J Biol Chem*. 2003; 278: 34427–37.
35. **Dickinson LA, Edgar AJ, Ehley J, *et al*.** Cyclin L is an RS domain protein involved in pre-mRNA splicing. *J Biol Chem*. 2002; 277: 25465–73.
36. **Wozniak MA, Kwong L, Chodniewicz D, *et al*.** R-Ras controls membrane protrusion and cell migration through the spatial regulation of Rac and Rho. *Mol Biol Cell*. 2005; 16: 84–96.
37. **Ma S, Huang J.** Regularized gene selection in cancer microarray meta-analysis. *BMC Bioinformatics*. 2009. doi:10.1186/1471-2105-10-1.
38. **Yamasaki S, Stoecklin G, Kedersha N, *et al*.** T-cell intracellular antigen-1 (TIA-1)-induced translational silencing promotes

the decay of selected mRNAs. *J Biol Chem*. 2007; 282: 30070–7.
39. **Anderson P, Kedersha N.** Stress granules: the Tao of RNA triage. *Trends Biochem Sci*. 2008; 33: 141–50.
40. **MacNicol AM, Wilczynska A, MacNicol MC.** Function and regulation of the mammalian Musashi mRNA translational regulator. *Biochem Soc Trans*. 2008; 36: 528–30.
41. **Dobson NR, Zhou YX, Flint NC, *et al*.** Musashi1 RNA-binding protein regulates oligodendrocyte lineage cell differentiation and survival. *Glia*. 2008; 56: 318–30.
42. **Siddall NA, McLaughlin EA, Marriner NL, *et al*.** The RNA-binding protein Musashi is required intrinsically to maintain stem cell identity. *Proc Nat Acad Sci USA*. 2006; 103: 8402–7.
43. **Wang XY, Yin Y, Yuan H, *et al*.** Musashi1 modulates mammary progenitor cell expansion through proliferin-mediated activation of the Wnt and Notch pathways. *Mol Cell Biol*. 2008; 28: 3589–99.
44. **Gartel AL, Tyner AL.** The role of the cyclin-dependent kinase inhibitor p21 in apoptosis. *Mol Cancer Therapeutics*. 2002; 1: 639–49.
45. **Philipp-Staheli J, Payne SR, Kemp CJ.** p27(Kip1): regulation and function of a haploinsufficient tumor suppressor and its misregulation in cancer. *Exp Cell Res*. 2001; 264: 148–68.
46. **King KL, Cidlowski JA.** Cell cycle and apoptosis: common pathways to life and death. *J Cell Biochem*. 1995; 58: 175–80.
47. **Meikrantz W, Schlegel R.** Apoptosis and the cell cycle. *J Cell Bioch*. 1995; 58: 160–74.
48. **Meikrantz W, Gisselbrecht S, Tam SW, *et al*.** Activation of cyclin A-dependent protein kinases during apoptosis. *Proc Nat Acad Sci USA*. 1994; 91: 3754–8.
49. **Shi TP, Xu H, Wei JF, *et al*.** Association of low expression of notch-1 and jagged-1 in human papillary bladder cancer and shorter survival. *J Urol*. 2008; 180: 361–6.
50. **Thomas MG, Martinez Tosar LJ, Desbats MA, *et al*.** Mammalian Staufen 1 is recruited to stress granules and impairs their assembly. *J Cell Sci*. 2009; 122: 563–73.
51. **Arimoto K, Fukuda H, Imajoh-Ohmi S, Saito H, *et al*.** Formation of stress granules inhibits apoptosis by suppressing stress-responsive MAPK pathways. *Nature Cell Biol*. 2008; 10: 1324–32.
52. **Wu Q, Hoffmann MJ, Hartmann FH, *et al*.** Amplification and overexpression of the ID4 gene at 6p22.3 in bladder cancer. *BMC Mol Cancer*. 2005. doi:10.1186/1476-4598-4-16.